



A CAAX motif can compensate for the PH domain of Num1 for cortical dynein attachment

Item Type	Article
Authors	Tang, Xianying;Punch, Jesse J.;Lee, Wei-Lih
DOI	10.4161/cc.8.19.9731
Download date	2026-06-12 11:32:07
Link to Item	https://hdl.handle.net/20.500.14394/3990



A CAAX motif can compensate for the PH domain of Num1 for cortical dynein attachment

Xianying Tang, Jesse J. Punch & Wei-Lih Lee

To cite this article: Xianying Tang, Jesse J. Punch & Wei-Lih Lee (2009) A CAAX motif can compensate for the PH domain of Num1 for cortical dynein attachment, *Cell Cycle*, 8:19, 3182-3190, DOI: [10.4161/cc.8.19.9731](https://doi.org/10.4161/cc.8.19.9731)

To link to this article: <https://doi.org/10.4161/cc.8.19.9731>



Published online: 01 Oct 2009.



Submit your article to this journal [↗](#)



Article views: 499



View related articles [↗](#)



Citing articles: 3 View citing articles [↗](#)

A CAAX motif can compensate for the PH domain of Num1 for cortical dynein attachment

Xianying Tang, Jesse J. Punch and Wei-Lih Lee*

Biology Department; University of Massachusetts at Amherst; Amherst, MA USA

Keywords: cytoplasmic dynein, cortical dynein, spindle orientation, PH domain, CAAX motif, PIP2

During mitosis in budding yeast, cortically anchored dynein exerts pulling forces on cytoplasmic microtubules, moving the mitotic spindle into the mother-bud neck. Anchoring of dynein requires the cortical patch protein Num1, which is hypothesized to interact with PI(4,5)P₂ via its C-terminal pleckstrin homology (PH) domain. Here we show that the PH domain and PI(4,5)P₂ are required for the cortical localization of Num1, but are not sufficient to mediate the cortical assembly of Num1 patches. A GFP fusion to the PH domain localizes to the cortex in foci containing ~2 molecules, whereas patches of full-length Num1-GFP contain ~14 molecules. A membrane targeting sequence containing the CAAX motif from the yeast Ras2 protein can compensate for the PH domain to target Num1 to the plasma membrane as discrete patches. The CAAX-targeted Num1 exhibits overlapping but largely distinct localization from wild-type Num1. However, it is fully functional in the dynein pathway. More importantly, cortical PI(4,5)P₂ is dispensable for the localization and function of the CAAX-targeted Num1. Together, these results demonstrate that cortical assembly of Num1 into functional dynein-anchoring patches is independent of its interaction with PI(4,5)P₂.

Introduction

Movement and positioning of the mitotic spindle occurs through interactions between the distal tips of astral microtubules and the cell cortex. The minus-end directed microtubule motor, cytoplasmic dynein, plays a pivotal role in these microtubule-cortex interactions, as evidenced by studies in diverse organisms such as early embryo development in *C. elegans*,¹⁻³ germline stem cell divisions in *D. melanogaster*,⁴ nuclear migration in *A. nidulans* and *S. cerevisiae*,⁵⁻⁹ and spindle alignment in cultured mammalian cells.¹⁰⁻¹² The general hypothesis emerging from these studies is that astral microtubules probe the cell cortex for dynein attachment sites; anchored dynein then generates pulling forces on the microtubule, causing the spindle to orient or move to a defined position. Although various studies have implicated dynein in generating force between microtubules and the cell cortex, the mechanism by which dynein is attached at the cortex is poorly understood.

In the budding yeast *S. cerevisiae*, cortical attachment of dynein requires the nuclear migration protein Num1.^{5,7,13,14} The *NUM1* gene encodes a 313 kDa protein consisting of a predicted N-terminal coiled-coil domain, a predicted EF hand, a central region that contains thirteen repeats of 64 amino acids of unknown function, and a C-terminal pleckstrin homology (PH) domain (Suppl. Fig. 1 and ref. 15). Num1 associates with dynein^{14,16} and localizes to the plasma membrane as discrete non-motile patches.^{7,13} A favored hypothesis is that Num1 anchors dynein to the cortex through the interaction between its PH

domain and PI(4,5)P₂ at the plasma membrane, since the PH domain binds tightly to PI(4,5)P₂ in vitro.¹⁷ However, whether the interaction with PI(4,5)P₂ mediates the assembly of Num1 into stationary cortical patches has not been directly tested. More importantly, it is not known whether this interaction is required for Num1 to mediate anchoring of cortical dynein.

In this study, we found that although the PH-PI(4,5)P₂ interaction is required for targeting of Num1 to the cell cortex, it is not sufficient to mediate formation of cortical patches characteristic of full-length Num1. Using a membrane targeting sequence from the yeast Ras2 protein, we showed that Num1 targeted to the cell cortex via an entirely different mechanism is fully functional in the dynein pathway, indicating that the sole role of the PH domain is to direct membrane targeting.

Results

PH domain alone is not sufficient for assembly of cortical Num1 patches. We asked whether the C-terminal PH domain of Num1 is sufficient for Num1 targeting to the plasma membrane as discrete patches. We altered the *NUM1* locus to express only the PH domain fused with GFP under its native promoter. Two different PH domain boundaries were tested: (1) amino acids 2574–2683 as defined by the Pfam database,¹⁸ and (2) amino acids 2563–2692 as defined by a genome-wide study of PH domains in *S. cerevisiae*.¹⁷ Haploid cells carrying the Pfam-defined *PH*₍₂₅₇₄₋₂₆₈₃₎-GFP exhibited diffuse cytoplasmic fluorescence and no cortical localization. However, haploid cells carrying *PH*₍₂₅₆₃₋₂₆₉₂₎-GFP

*Correspondence to: Wei-Lih Lee; Email: wlee@bio.umass.edu

Submitted: 07/23/09; Accepted: 08/04/09

Previously published online: www.landesbioscience.com/journals/cc/article/9731

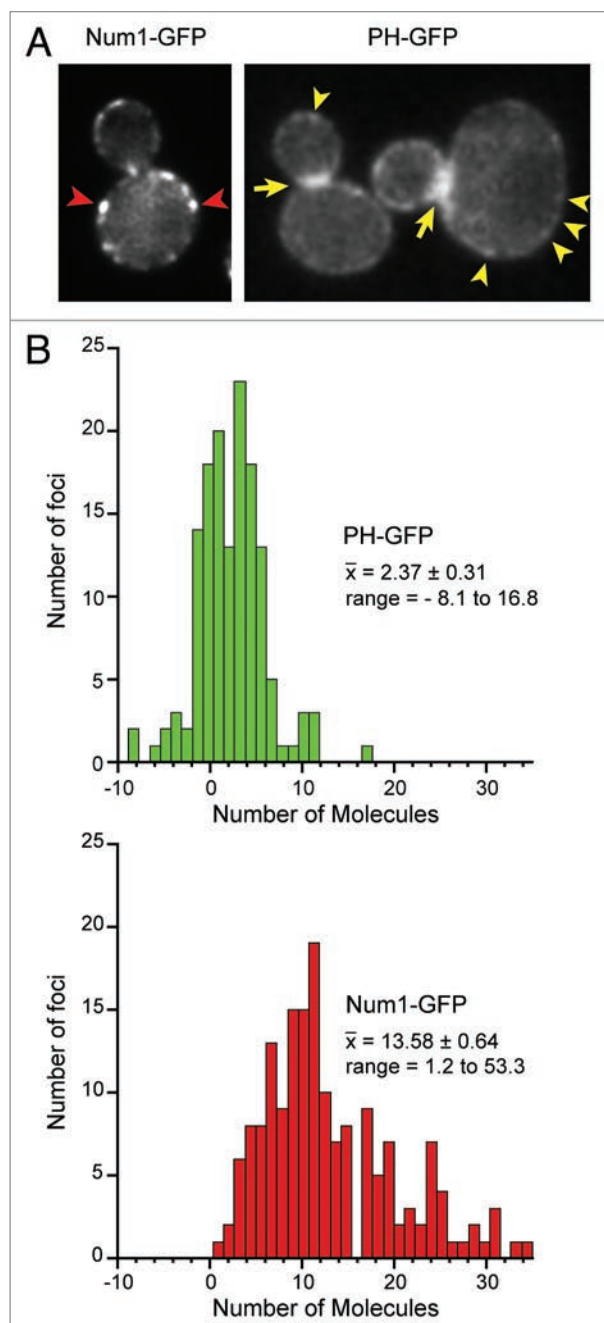


Figure 1. Localization of full-length Num1 and isolated PH domain. (A) Wide-field single focal plane images of live cells expressing Num1-GFP (left) or PH-GFP (right; construct No. 8 in Fig. 2) at the *NUM1* chromosomal locus under the control of the *NUM1* promoter. Arrowheads indicate representative bright and dim Num1-GFP and PH-GFP foci, respectively. Arrows indicate enhanced PH-GFP signal at the bud neck. (B) Histograms of the number of molecules of PH-GFP and Num1-GFP per cortical focus. The fluorescence intensity of individual foci of PH-GFP ($n = 143$), Num1-GFP ($n = 173$) and Cse4-GFP ($n = 184$) was measured using ImageJ. The mean intensity of Cse4-GFP foci (Suppl. Fig. 2) was used as a standard to normalize the intensity of PH-GFP and Num1-GFP to number of molecules. Values less than zero are a result of background subtraction.

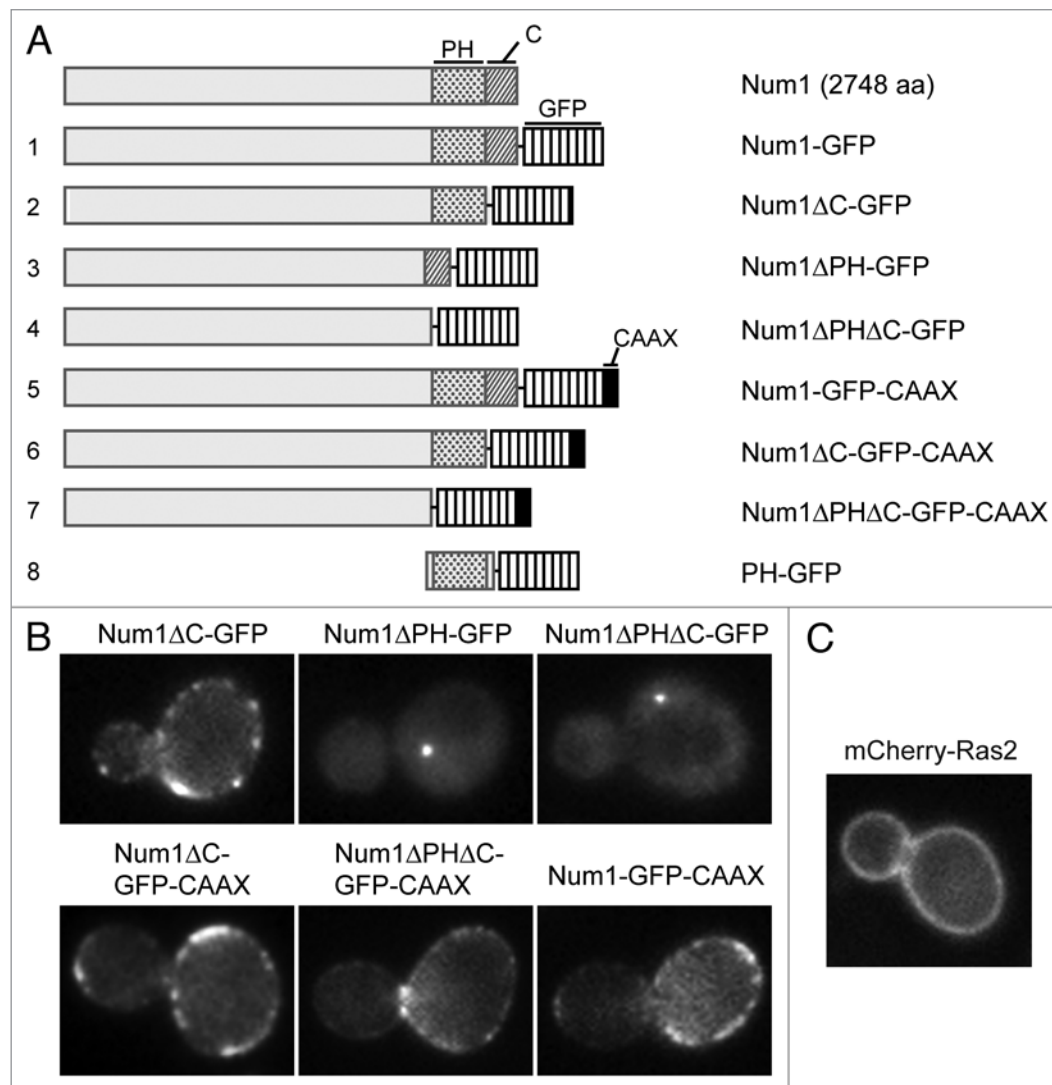
exhibited discrete cortical foci along the mother and daughter cell cortex (Fig. 1A, right, arrowheads), as previously described for full-length Num1-GFP foci.^{7,14} We also found that PH₍₂₅₆₃₋₂₆₉₂₎-GFP showed enhanced signal at the bud neck region (Fig. 1A, right, arrows), a localization pattern that was similarly observed when the PH domain of rat phospholipase PLC- δ 1 was expressed in yeast cells as a GFP fusion protein.¹⁹ The discrepancy between PH₍₂₅₆₃₋₂₆₉₂₎-GFP and the Pfam-defined PH₍₂₅₇₄₋₂₆₈₃₎-GFP suggests that the former contains the minimal PH domain required for proper folding and interactions with the cortical membrane.

We observed significant differences between the cortical foci of PH₍₂₅₆₃₋₂₆₉₂₎-GFP (hereafter referred to as PH-GFP) and full-length Num1-GFP. Most notably, the fluorescence intensity of individual foci is lower for PH-GFP than Num1-GFP (Fig. 1A). PH-GFP cells did not contain bright foci that were frequently observed in *NUM1*-GFP cells (Fig. 1A, left, arrowheads). Using quantitative ratiometric methods, we determined the number of fluorescent molecules at individual cortical foci. Cse4, a stable kinetochore protein present at two copies per chromosome,^{20,21} was used as a standard for the intensity measurements (Suppl. Fig. 2). We found that on average, cortical PH-GFP foci contain ~2 molecules per focus (Fig. 1B, top). The intensities of full-length Num1-GFP foci gave a broader distribution with a mean of ~14 molecules per focus (Fig. 1B, bottom). Immunoblot analysis revealed that the dimmer patch formed by PH-GFP was not due to unstable protein (Suppl. Fig. 3). These results indicate that the PH domain is not sufficient to mediate the full assembly of cortical Num1 patches.

PH domain is required for plasma membrane targeting. Next, we asked whether the PH domain is necessary for Num1 localization to the plasma membrane. In previous studies, Num1 constructs lacking the PH domain were found diffusely in the cytoplasm and did not localize to the cell cortex. However, these studies used constructs that contained either (1) a large C-terminal deletion,¹⁴ or (2) a deletion that included internal and C-terminal sequences,¹³ or (3) a deletion that included the PH domain and the last 65 amino acids of Num1,²² referred to here as “C domain” (Fig. 2A), which contains multiple predicted PKA and PKC phosphorylation sites.¹⁵ Thus, a strict requirement for the PH domain in cortical targeting of Num1 has not been firmly established.

We performed targeted disruption of the PH domain. We altered the *NUM1* locus to express truncated Num1 constructs lacking the PH domain, the C domain, or both PH and C domains, each fused with GFP under the control of its native promoter (Fig. 2A). Deleting the PH domain or the C domain or both did not result in unstable proteins (Suppl. Fig. 3). In fact, Num1 appeared more stable when the PH and C domains were deleted. Haploid cells carrying *num1 Δ C-GFP* as their sole source of Num1 exhibited cortical foci indistinguishable from full-length Num1-GFP foci (Fig. 2B), indicating that the C domain is not required for cortical patch assembly. In contrast, haploid cells carrying *num1 Δ PH-GFP* or *num1 Δ PH Δ C-GFP* did not exhibit cortical foci, in agreement with a role of the PH domain in cortical targeting.^{13,14} Interestingly, we observed that Num1 Δ PH-GFP and Num1 Δ PH Δ C-GFP constructs were present as motile

Figure 2. Chimeric Num1 containing the CAAX motif of Ras2 in place of the PH domain localizes to the cell cortex as discrete foci. (A) Schematic representation of Num1 constructs used in this study. The PH domain (residues 2574–2683), C domain (residues 2684–2748), GFP tag, and CAAX motif are as indicated. For construct 3 and 8, residues 2563–2692 encompassing the PH domain were either deleted or expressed alone as a GFP fusion, respectively. (B) Wide-field single focal plane images of living cells expressing the indicated constructs at the *NUM1* chromosomal locus under the control of the *NUM1* promoter. (C) Live cell expressing N-terminally tagged mCherry-Ras2 expressed from a CEN-plasmid under the control of the *RAS2* promoter.



foci in the cytoplasm, with the number of foci per cell ranging from one to three (Fig. 2B; Video 1). This pattern is distinct from the diffuse cytoplasmic localization previously reported for Num1 fragments lacking the PH domain.¹⁵ The localization of Num1ΔPH-GFP and Num1ΔPHΔC-GFP to cytoplasmic foci may be due to their association with mitochondria via an interaction with the dynamin-related Dnm1 protein.²³ We stained the mitochondria in *num1ΔPH-GFP* and *num1ΔPHΔC-GFP* cells with mitotracker and found that the motile cytoplasmic foci of Num1ΔPH-GFP and Num1ΔPHΔC-GFP co-localized with mitochondrial tubules (Videos 2 and 3). These results show that the PH domain is required for cortical targeting of Num1, but not for its association with mitochondria.

CAAX motif in place of the PH domain restores cortical localization. To test whether the PH domain is only required for recruitment of Num1 to the cortex, we replaced the PH domain with a different membrane targeting sequence. We fused the membrane-targeting sequence of Ras2, GSGGCCIIIS, to the C-terminus of Num1ΔPHΔC-GFP. These nine amino acids located at the C-terminus of Ras2 (hereafter referred to as CAAX motif) signal for prenylation and palmitoylation^{24,25}

and have previously been used to direct cytoplasmic proteins to the plasma membrane.²⁶ Haploid cells carrying *num1ΔPHΔC-GFP-CAAX* as the only source of Num1 exhibited discrete cortical foci similar to those observed in *NUM1-GFP* cells (Fig. 2B). Quantitative measurements showed that the intensities of Num1ΔPHΔC-GFP-CAAX foci were lower compared to Num1-GFP foci, but they were significantly higher than PH-GFP foci. On average, cortical Num1ΔPHΔC-GFP-CAAX foci contained ~9 molecules per focus (Fig. 3A). This was ~1.5-fold lower than full-length Num1-GFP foci, but ~4-fold higher than PH-GFP foci (Fig. 3B). As a control, we examined the localization of Ras2, the protein from which we obtained the CAAX motif. Cells expressing N-terminally tagged mCherry-Ras2, under the control of its native promoter, showed evenly distributed fluorescence along the plasma membrane (Fig. 2C). Additionally, as for Num1-GFP foci,⁷ we found that Num1ΔPHΔC-GFP-CAAX foci appeared to be stationary during time-lapse image collections (10–15 min duration). These results demonstrate that attaching a C-terminal CAAX motif enables Num1ΔPHΔC-GFP to assemble into cortical patches that are similar to Num1-GFP.

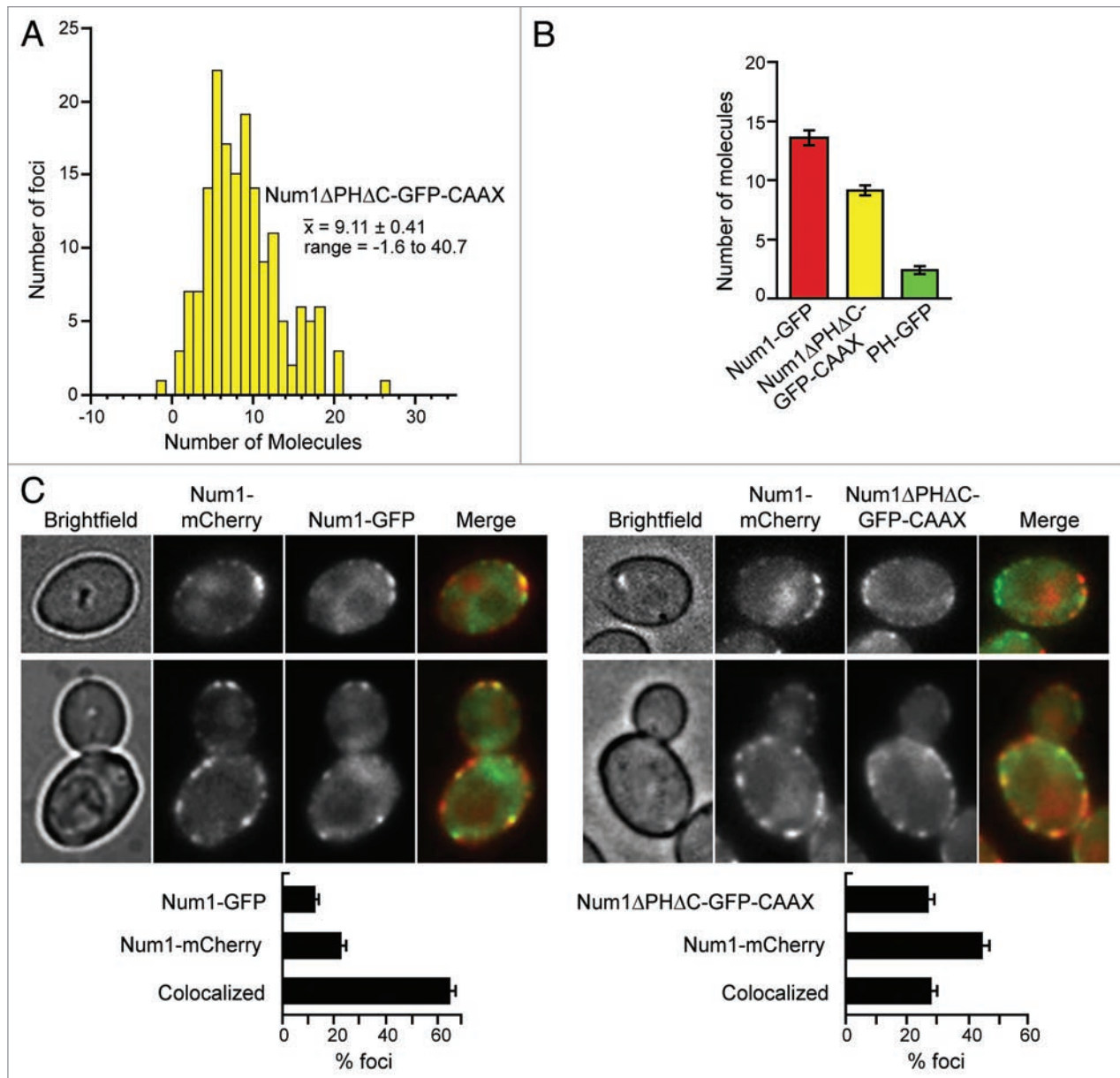


Figure 3. Targeting of Num1 Δ PH Δ C-GFP-CAAX versus Num1-GFP. (A) Histogram of the number of molecules of Num1 Δ PH Δ C-GFP-CAAX per cortical focus ($n = 168$). (B) Mean number of molecules of Num1-GFP, Num1 Δ PH Δ C-GFP-CAAX and PH-GFP per cortical focus. Error bars represent standard error. (C) Num1-GFP and Num1 Δ PH Δ C-GFP-CAAX show overlapping but distinct cortical localization in the same cell. *Left*: diploid cells carrying *NUM1-mCherry* and *NUM1-GFP*. *Right*: diploid cells carrying *NUM1-mCherry* and *num1 Δ PH Δ C-GFP-CAAX*. Merged images show Num1-mCherry in red and Num1-GFP and Num1 Δ PH Δ C-GFP-CAAX in green. Bottom panel shows the percentage of foci exhibiting signals for GFP only, mCherry only, or both. Bars represent standard error of proportion; $n = 400$ for each.

Num1 Δ PH Δ C-GFP-CAAX foci overlap with but are distinct from those of wild-type Num1. To test whether Num1 Δ PH Δ C-GFP-CAAX localized to the same cortical sites as full-length Num1, we constructed a diploid strain carrying *num1 Δ PH Δ C-GFP-CAAX* and *NUM1-mCherry* at the two *NUM1* chromosomal loci, both under the control of the native *NUM1* promoter. Imaging of the resulting diploid strain revealed that Num1-mCherry and Num1 Δ PH Δ C-GFP-CAAX often localized to distinct foci: ~45% of cortical foci had only Num1-mCherry,

~27% had only Num1 Δ PH Δ C-GFP-CAAX, and ~28% had both ($n = 400$ foci; Fig. 3C, right). Conversely, imaging of a control diploid strain carrying *NUM1-mCherry* and *NUM1-GFP* at the two *NUM1* chromosomal loci revealed that the majority of Num1-mCherry and Num1-GFP fluorescence colocalized at the same foci: ~22% of cortical foci had only Num1-mCherry, ~13% had only Num1-GFP, and ~65% had both ($n = 400$ foci; Fig. 3C, left). Thus, these results showed that Num1 Δ PH Δ C-GFP-CAAX assembles at cortical sites that are distinct from those of wild-type Num1.

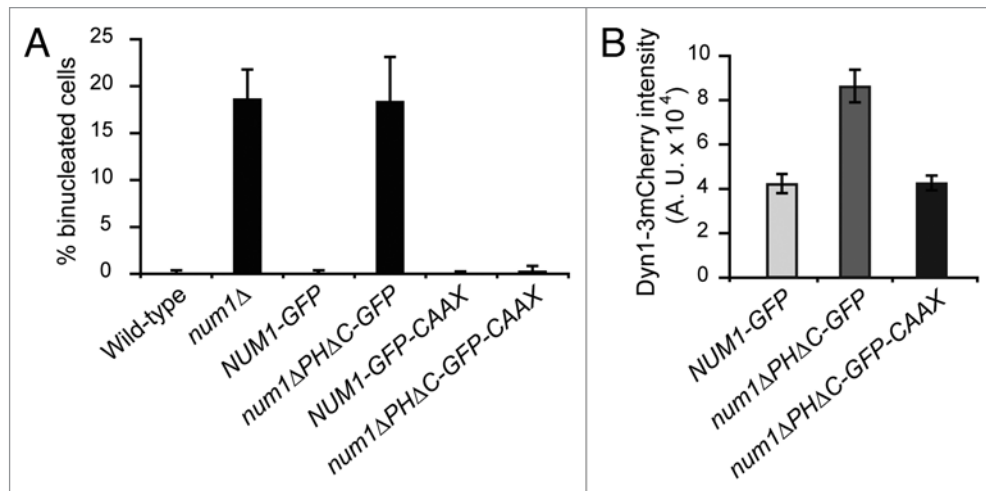


Figure 4. CAAX rescues *num1ΔPHΔC-GFP* function in the dynein pathway. (A) Percentage of binucleated cells in indicated strains. Mid-log cultures were shifted to 12°C for ~16 h, fixed and stained for nuclei with DAPI, and imaged. The percentage of binucleated cells was plotted for each strain. Error bars represent standard deviation ($n > 1000$ cells for each strain). (B) Fluorescence intensity of plus end Dyn1-3mCherry foci in strains carrying *NUM1-GFP*, *num1ΔPHΔC-GFP* and *num1ΔPHΔC-GFP-CAAX*. Each strain also expressed CFP-Tub1 to mark microtubules. A 2 μm Z-stack of images was collected at 5 s intervals for Dyn1-3mCherry and CFP-Tub1. Motile plus end foci of Dyn1-3mCherry were identified and measured as described.¹⁶ Error bars represent standard error ($n > 40$ plus end foci for each strain).

Num1ΔPHΔC-GFP-CAAX is functional in the dynein pathway. We next evaluated Num1ΔPHΔC-GFP-CAAX for dynein pathway function. Loss of *NUM1* causes a nuclear segregation phenotype characterized by accumulation of cells with two nuclei in the mother (binucleate cells). This phenotype is enhanced at low temperatures.²⁷⁻²⁹ Figure 4A shows that, after incubation at 12°C, ~18.7% of *num1Δ* cells exhibited a binucleate phenotype, whereas only 0.1% of wild-type and *NUM1-GFP* cells exhibited a binucleate phenotype. As expected from the loss of cortical localization (Fig. 2B, top row, third from left), ~18.4% of *num1ΔPHΔC-GFP* cells exhibited a binucleate phenotype, similar to that of a *num1Δ* mutant. Strikingly, when the CAAX sequence was fused to *num1ΔPHΔC-GFP*, the percentage of binucleate cells was reduced to 0.4%, indicating that the CAAX motif fully restored the nuclear segregation function of Num1ΔPHΔC-GFP.

We further examined the function of Num1ΔPHΔC-GFP-CAAX by assaying for rescue of synthetic growth defects with the Kar9 pathway. Budding yeast need either the dynein or Kar9 pathway for normal growth.³⁰⁻³³ Tetrad analysis showed that *num1Δ kar9Δ* double mutants (12 of 12) formed microcolonies that grew poorly (Table 1). In contrast, *num1ΔPHΔC-GFP-CAAX kar9Δ* double mutants grew normally (10 of 10), forming colonies that were indistinguishable from those of wild-type or parental single mutants, indicating that Num1ΔPHΔC-GFP-CAAX rescued the synthetic growth defects with *kar9Δ*. In control crosses, *num1ΔPHΔC-GFP kar9Δ* double mutants formed microcolonies (11 of 11), whereas *NUM1-GFP kar9Δ* (12 of 12) and *NUM1-GFP-CAAX kar9Δ* (12 of 12) progeny formed normal colonies with no observable growth defects.

To investigate the rescue of dynein function more directly, we evaluated how Num1ΔPHΔC-GFP and Num1ΔPHΔC-GFP-CAAX affect cortical attachment of dynein heavy chain Dyn1/

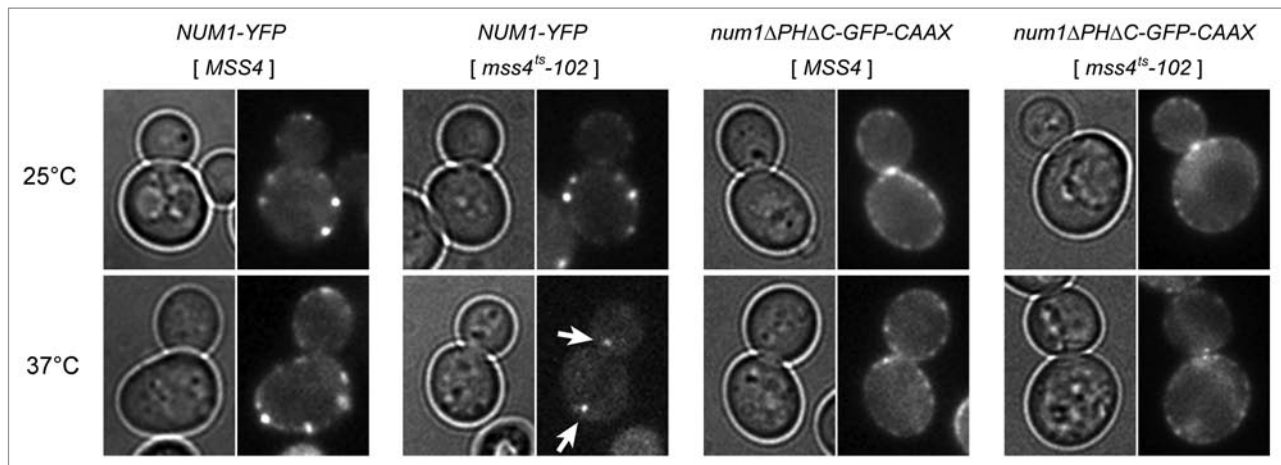
HC. We previously showed that Dyn1/HC is targeted to motile foci at the plus end of cytoplasmic microtubules, and to stationary foci at the cell cortex, which we proposed represent cortically anchored dynein.³⁰ We found that *num1Δ* cells (Video 4) and *num1ΔPHΔC-GFP* cells (Video 6) exhibited plus end foci but no cortical foci of Dyn1/HC-3mCherry. In contrast, *num1ΔPHΔC-GFP-CAAX* cells exhibited both plus end and cortical foci of Dyn1/HC-3mCherry (Video 7), similar to those observed in a control *NUM1-GFP* strain (Video 5). Additionally, we examined how Num1ΔPHΔC-GFP and Num1ΔPHΔC-GFP-CAAX affect the level of Dyn1/HC-3mCherry at the plus end of cytoplasmic microtubules. Loss of cortical attachment of Dyn1/HC leads to an enhanced level of Dyn1/HC at the plus ends.^{31,34} We found that the intensity of Dyn1/HC-3mCherry at the plus ends in *num1ΔPHΔC-GFP* cells was higher than that in *num1ΔPHΔC-GFP-CAAX* cells (Fig. 4B), which showed a level similar to wild-type cells. Thus, cortical attachment of dynein was rescued in *num1ΔPHΔC-GFP-CAAX* cells. Taken together, these results show that Num1ΔPHΔC-GFP-CAAX performs normal dynein pathway function.

Localization and function of Num1ΔPHΔC-GFP-CAAX is independent of PI(4,5)P₂. The PH domain of Num1 binds PI(4,5)P₂ in vitro with high affinity and specificity,¹⁷ suggesting that in the cell, interactions with PI(4,5)P₂ may help anchor Num1 to the cortex. To examine whether PI(4,5)P₂ affects the localization and function of Num1ΔPHΔC-GFP-CAAX, we altered PI(4,5)P₂ levels using *mss4^{ts}-102*, a temperature sensitive mutant of the essential PI(4)P 5-kinase *MSS4*. *Mss4* is responsible for all PI(4,5)P₂ synthesis at the plasma membrane.³⁵⁻³⁷ Heat inactivation of *mss4^{ts}-102* causes significant reduction in PI(4,5)P₂ levels (to <20% of wild-type levels) without affecting the levels of other phosphoinositide species.³⁷ We constructed *NUM1-YFP mss4Δ* and *num1ΔPHΔC-GFP-CAAX mss4Δ* strains

Table 1. Viability of *NUM1* alleles in combination with *kar9Δ* mutant

Mutant crossed with <i>kar9Δ</i>	Number of tetrads analyzed	Number of predicted double mutants	Viability of double mutant	
			Microcolony	Viable
<i>num1Δ</i>	11	12	12	-
<i>NUM1-GFP</i>	12	12	-	12
<i>num1ΔPHΔC-GFP</i>	11	11	11	-
<i>NUM1-GFP-CAAX</i>	12	12	-	12
<i>num1ΔPHΔC-GFP-CAAX</i>	12	10	-	10

Indicated mutant strains were crossed with *kar9Δ*. The resulting diploid strains were sporulated, and tetrads were dissected.



Do not distribute.

Figure 5. Inactivation of *Mss4* results in loss of cortical *Num1-YFP*, but not *Num1ΔPHΔC-GFP-CAAX*. *NUM1-YFP* and *num1ΔPHΔC-GFP-CAAX* strains carrying chromosomal *mss4Δ* and either *MSS4* plasmid or *mss4^{ts}-102* plasmid were cultured at 25°C to mid-log phase and then shifted to 37°C for 2 h 20 min prior to fluorescence microscopy. Bright field and single focal plane wide-field images of live cells are shown. Arrows indicate motile cytoplasmic *Num1-YFP* foci (see Video 8) observed after inactivation of *mss4^{ts}-102*.

harboring the conditional *mss4^{ts}-102* or wild-type *MSS4* plasmid. At the permissive temperature (25°C), *NUM1-YFP* and *num1ΔPHΔC-GFP-CAAX* cells expressing *mss4^{ts}-102* as their only source of *Mss4* exhibited cortical foci that were indistinguishable from those expressing *MSS4* (Fig. 5). After shifting to the restrictive temperature (37°C), we found that ~68% (n = 251) of *NUM1-YFP* cells expressing *mss4^{ts}-102* exhibited a loss of cortical *Num1-YFP* foci; the majority of these cells had one to three motile cytoplasmic foci (Fig. 5, arrows; Video 8) that were strikingly similar to those observed in *num1ΔPHΔC-GFP* cells (Video 1; Fig. 2B, top row, third from left). In contrast, after an identical temperature shift, we observed that all *num1ΔPHΔC-GFP-CAAX* cells expressing *mss4^{ts}-102* (n = 261) exhibited cortical foci that were indistinguishable from those in pre-shifted cells (Fig. 5). Similarly, cortical foci in *NUM1-YFP* (n = 571) and *num1ΔPHΔC-GFP-CAAX* (n = 525) cells harboring the control *MSS4* plasmid were unaffected by the temperature shift (Fig. 5). These findings demonstrate that cortical targeting of *Num1ΔPHΔC-GFP-CAAX* does not depend on $PI(4,5)P_2$ levels at the cell cortex.

To assess dynein function after inactivation of *Mss4*, we scored for dynein-dependent spindle oscillation across the bud neck, using a *kar9Δ* background to enhance spindle movements.³⁸ We

found that *NUM1-YFP mss4Δ kar9Δ* cells expressing *mss4^{ts}-102* as their only source of *Mss4* showed a large decrease in spindle oscillation events after shifting to the restrictive temperature (pre-shift: 81.4% of spindles, n = 97; after-shift: 57.3% of spindles, n = 89). In comparison, *num1ΔPHΔC-GFP-CAAX mss4Δ kar9Δ* cells expressing *mss4^{ts}-102* showed a much smaller decrease in spindle oscillation events after an identical temperature shift (pre-shift: 82.5% of spindles, n = 114; after-shift: 72.2% of spindles, n = 90). These spindle oscillations often coincided with lateral sliding of a cytoplasmic microtubule along the cell cortex, indicating cortical dynein activity (Video 9). Thus, these results indicate that the function of *Num1ΔPHΔC-GFP-CAAX* does not depend on $PI(4,5)P_2$ levels at the cell cortex.

Discussion

In summary, we found that the interaction between the PH domain and $PI(4,5)P_2$ directs plasma membrane targeting but is not sufficient to mediate cortical patch assembly of *Num1*. Our analysis of CAAX-targeted constructs lacking the PH domain indicates that membrane targeting by the PH domain can be substituted by a different mechanism, and yet, *Num1* remains fully functional for dynein anchoring. Furthermore, we discovered

that Num1 Δ PH Δ C-GFP-CAAX assembles patches at sites distinguishable from those of wild-type Num1, suggesting that there may be no preferential sites at the cell cortex for Num1 to exert its function in spindle positioning.

Num1 is an essential component of the dynein pathway, which mediates timely and efficient movement of the mitotic spindle into the bud neck during mitosis.^{7,39,40} One important question regarding Num1 function is how it is tethered at the plasma membrane to form a functional platform for anchoring dynein. Although previous studies have implicated its PH domain in membrane targeting, the manner in which this domain contributes to Num1 patch assembly was unclear. Our data reveal that PH-GFP foci are significantly dimmer than full-length Num1-GFP foci (Fig. 1). Molecule-counting indicates that there are only ~2 molecules of PH-GFP per cortical focus, compared to ~14 molecules per cortical focus for full-length Num1-GFP. This result, together with our deletion analysis (Num1 Δ PH-GFP, Num1 Δ C-GFP and Num1 Δ PH Δ C-GFP; Fig. 2), suggests that the sole function of the PH domain is to mediate the recruitment of Num1 to the cell cortex. We propose that an additional step of aggregation, which may be mediated by the sequence N-terminal to the PH domain, is required for Num1 to form functional patches. Consistent with this idea, we find that a CAAX motif is sufficient to replace the PH domain to form non-motile bright cortical foci when attached to the N-terminal sequence of Num1. In contrast, the Ras2 protein, which also contains a CAAX motif, localizes smoothly at the cell cortex.

Quite surprisingly, although Num1 Δ PH Δ C-GFP-CAAX shows largely distinct localization from wild-type Num1-mCherry (Fig. 3C), it is fully functional in the dynein pathway. Since both Num1- Δ PH Δ C-GFP-CAAX and Num1-GFP foci are non-motile, and both proteins share the same N-terminal sequence, we speculate that the N-terminal-sequence-mediated aggregation of Num1 is the key determinant in the formation of a stationary structural scaffold for dynein anchoring. For Num1-GFP, this scaffold binds tightly to the plasma membrane via numerous PH-PI(4,5)P₂ interactions. For Num1- Δ PH Δ C-GFP-CAAX, this scaffold is covalently attached to the cytoplasmic face of the plasma membrane via numerous hydrophobic palmitate and prenyl groups. It would be interesting to investigate in the future how the N-terminal sequence is involved in the patch assembly of Num1.

Materials and Methods

Yeast strains and plasmids. Yeast strains used in this study are listed in **Supplementary Table 1**. All strains are isogenic with YWL36,⁴¹ and were constructed by standard genetic cross or by PCR product-mediated transformation.⁴² Correct tagging of Num1 with GFP or GFP-CAAX was confirmed by sequencing the PCR product amplified from the tagged genomic locus. CEN-containing plasmids pRS416-*MSS4* and YCplac111-*mss4^{tr}-102* were recovered from strains AAY201 and AAY202, respectively.³⁷ The GFP-tagging vectors pKT0127 and pKT0128 were obtained from Addgene plasmid repository. We converted pKT0127 into a GFP-6xHIS-tagging vector, pXT07, by

ligating a synthetic insert made from two oligos with the sequence 5'-GTACAAAGATTACGATATCCCAACGCATCACCATCA CCATCACTA G-3' and 5'-GTACCTAGTGATGGTGATGGT GATGCGTTGGGATATCGTAATCTTT-3' into BsrGI-digested pKT0127.

To replace the chromosomal *NUM1* gene with *PH-GFP* sequence, we first built a targeting vector containing the *NUM1* upstream and downstream non-coding sequences. Briefly, a PCR fragment containing 400 bp downstream of the *NUM1* stop codon was amplified from genomic DNA using primers flanked with AatII sites and cloned into AatII-digested pRS304,⁴³ generating pXT10. Next, a fragment containing the GFP-6xHIS coding sequence was amplified from pXT07 using a forward primer flanked with BamHI and Sall sites and a reverse primer flanked with a BglII site. The PCR fragment was digested with BamHI and BglII and ligated into BamHI-digested pXT10, generating pXT12. Next, a PCR fragment containing 601 bp upstream of the *NUM1* start codon was amplified from genomic DNA using a forward primer flanked with a Sall site and a reverse primer flanked with a XhoI site. The PCR fragment was digested with Sall and XhoI and ligated into XhoI-digested pXT12, generating pXT15, the targeting vector that contains *NUM1* upstream and downstream non-coding sequences. The coding sequence of Num1 PH domain (residues 2563–2692)¹⁷ was amplified from genomic DNA using a forward primer flanked with a XhoI site and a reverse primer flanked with a Sall site. The PCR fragment was digested with XhoI and Sall and ligated into XhoI/Sall-digested pXT15, generating pXT33. Pfam-defined PH domain (residues 2574–2683) was cloned similarly into XhoI/Sall-digested pXT15, generating pXT21. To construct the *PH*₍₂₅₆₃₋₂₆₉₂₎-GFP and *PH*₍₂₅₇₄₋₂₆₈₃₎-GFP strains, pXT33 and pXT21 were digested with AvrII and MluI, and the resulting 4.1 kb fragment was gel purified and transformed into a *num1* Δ strain (YWL555).

To replace the chromosomal *NUM1* gene with *num1* Δ PH-GFP sequence, we constructed pXT38. Briefly, a XhoI/BamHI fragment containing the coding sequence of *NUM1* without the stop codon was cloned into XhoI/BamHI-digested pXT12, generating pXT12-*NUM1-no-stop-codon*. We verified the entire *NUM1* coding sequence by DNA sequencing. Next, a PCR fragment containing 601 bp upstream of the *NUM1* start codon was amplified from genomic DNA using a forward primer flanked with a Sall site and a reverse primer flanked with a XhoI site. The PCR fragment was digested with Sall and XhoI and ligated into XhoI-digested pXT12-*NUM1-no-stop-codon*, generating pXT19. Next, using a PCR-based technique for joining DNA sequences,⁴⁴ we amplified from pXT19 the sequences flanking the PH domain (encompassed by two NdeI sites) as one 0.9 kb NdeI fragment. The resulting PCR product was digested with NdeI and ligated into NdeI-digested pXT19, generating pXT38. To construct *num1* Δ PH-GFP strain, pXT38 was digested with AvrII and MluI, and the resulting 11.6 kb fragment, containing the coding sequence of *num1* Δ PH-GFP flanked by *NUM1* 5'-UTR and 3'-UTR sequences, was gel purified and transformed into a *num1* Δ strain (YWL555) to yield YWL1105.

To construct a vector for tagging Num1 with GFP-CAAX, pKT0128 was digested with BsrGI and ligated with a synthetic insert made from two oligos with the sequence 5'-GTACAAAGGTGCTGGTGCTGGATCGGGTGGCTGTTGTATTATAAGTTAA-3' and 5'-GTA CT TAACTTATAA TACAACAGCCACCCGATCCAGCACCAGCACCTTT-3'. The insert encodes a Gly-Ala-Gly-Ala linker followed by the C-terminal membrane-targeting sequence from Ras2, Gly-Ser-Gly-Gly-Cys-Cys-Ile-Ile-Ser.²⁶ The resulting plasmid pKT0128-RAS2-C-term was used as a template for PCR to tag *NUM1* at the chromosomal locus with GFP-CAAX.

To express mCherry-tagged Ras2, we amplified the mCherry open reading frame without the stop codon from pRS305-mCherry with a forward primer flanked with an AvrII site and a reverse primer flanked with a SpeI site and ligated the PCR fragment into a TOPO TA vector (Invitrogen). Next, we excised the mCherry fragment from the TOPO TA vector by AvrII and SpeI digestion and ligated it into SpeI-digested pRS315-MET3p, generating pRS315-MET3p-mCherry. A SpeI/SacI fragment containing the *RAS2* open reading frame amplified from genomic DNA was then cloned into the SpeI and SacI sites in pRS315-MET3p-mCherry, generating pRS315-MET3p-mCherry-RAS2. Finally, a Sall/BamHI fragment containing 795 bp immediately upstream of the *RAS2* open reading frame was amplified from genomic DNA and cloned into the Sall and BamHI sites in pRS315-MET3p-mCherry-RAS2, replacing the MET3p. The resulting plasmid, which expresses *mCherry-RAS2* under the control of *RAS2* promoter, was named pXT43.

References

- Gonczy P, Pichler S, Kirkham M, Hyman AA. Cytoplasmic dynein is required for distinct aspects of MTOC positioning, including centrosome separation, in the one cell stage *Caenorhabditis elegans* embryo. *J Cell Biol* 1999; 147:135-50.
- Schmidt DJ, Rose DJ, Saxton WM, Strome S. Functional analysis of cytoplasmic dynein heavy chain in *Caenorhabditis elegans* with fast-acting temperature-sensitive mutations. *Mol Biol Cell* 2005; 16:1200-12.
- Skop AR, White JG. The dynactin complex is required for cleavage plane specification in early *Caenorhabditis elegans* embryos. *Curr Biol* 1998; 8:1110-6.
- McGrail M, Hays TS. The microtubule motor cytoplasmic dynein is required for spindle orientation during germline cell divisions and oocyte differentiation in *Drosophila*. *Development* 1997; 124:2409-19.
- Bloom K. Nuclear migration: cortical anchors for cytoplasmic dynein. *Curr Biol* 2001; 11:326-9.
- Han G, Liu B, Zhang J, Zuo W, Morris NR, Xiang X. The *Aspergillus* cytoplasmic dynein heavy chain and NUDF localize to microtubule ends and affect microtubule dynamics. *Curr Biol* 2001; 11:719-24.
- Heil-Chapdelaine RA, Oberle JR, Cooper JA. The cortical protein Num1p is essential for dynein-dependent interactions of microtubules with the cortex. *J Cell Biol* 2000; 151:1337-44.
- Huisman SM, Segal M. Cortical capture of microtubules and spindle polarity in budding yeast—where's the catch? *J Cell Sci* 2005; 118:463-71.
- Xiang X, Han G, Winkelmann DA, Zuo W, Morris NR. Dynamics of cytoplasmic dynein in living cells and the effect of a mutation in the dynactin complex actin-related protein Arp1. *Curr Biol* 2000; 10:603-6.
- Ahringer J. Control of cell polarity and mitotic spindle positioning in animal cells. *Curr Opin Cell Biol* 2003; 15:73-81.

Fluorescence microscopy. Cells for fluorescence microscopy were cultured in synthetic defined media (SD) at 30°C unless stated otherwise. Cold nuclear segregation assay was performed as described.^{27,29,31} Briefly, early mid-log culture at 30°C was shifted to 12°C for 16 h, fixed with 70% ethanol and then stained with DAPI to visualize the nuclei. To examine movement of preanaphase spindles in YWL1472 and YWL1476 strains, cells were arrested in S phase at 25°C by addition of 200 mM hydroxyurea (HU) and then shifted to 37°C for 70 min. Spindle movement was visualized in live cells on agarose pads. Wide-field fluorescence images were collected using a 1.49 NA 100X objective on a Nikon 80i upright microscope equipped with SmartShutter (Sutter Instrument), motorized filter cube turret, and a cooled EM-CCD Cascade-II camera (Photometrics) controlled by the NIS-Elements software (Nikon). We used ImageJ to quantify fluorescence intensities of Num1 or Dyn1 foci as described.¹⁶

Acknowledgements

We thank Dr. Michele Klingbeil for aliquots of mitotracker. We are grateful to Steven Markus and Patricia Wadsworth for valuable discussions throughout this study. This work was supported by a University of Massachusetts Amherst Biology Department HHMI-sponsored Junior Fellowship to J.P., and an NIH/NIGMS grant (1R01GM076094) to W.-L.L.

Note

Supplementary materials can be found at:

www.landesbioscience.com/supplement/TancCC8-19-Sup.pdf

- O'Connell CB, Wang YL. Mammalian spindle orientation and position respond to changes in cell shape in a dynein-dependent fashion. *Mol Biol Cell* 2000; 11:1765-74.
- Siller KH, Doe CQ. Spindle orientation during asymmetric cell division. *Nat Cell Biol* 2009; 11:365-74.
- Farkasovsky M, Kuntzel H. Yeast Num1p associates with the mother cell cortex during S/G₂ phase and affects microtubule functions. *J Cell Biol* 1995; 131:1003-14.
- Farkasovsky M, Kuntzel H. Cortical Num1p interacts with the dynein intermediate chain Pac11p and cytoplasmic microtubules in budding yeast. *J Cell Biol* 2001; 152:251-62.
- Kormanec J, Schaaff-Gerstenschlager I, Zimmermann FK, Perecko D, Kuntzel H. Nuclear migration in *Saccharomyces cerevisiae* is controlled by the highly repetitive 313 kDa NUM1 protein. *Mol Gen Genet* 1991; 230:277-87.
- Markus SM, Punch JJ, Lee WL. Motor- and tail-dependent targeting of dynein to microtubule plus ends and the cell cortex. *Curr Biol* 2009; 19:196-205.
- Yu JW, Mendrola JM, Audhya A, Singh S, Keleti D, DeWald DB, et al. Genome-wide analysis of membrane targeting by *S. cerevisiae* pleckstrin homology domains. *Mol Cell* 2004; 13:677-88.
- Finn RD, Tate J, Mistry J, Coggill PC, Sammut SJ, Hotz HR, et al. The Pfam protein families database. *Nucleic Acids Res* 2008; 36:281-8.
- Mendoza M, Norden C, Durrer K, Rauter H, Uhlmann F, et al. A mechanism for chromosome segregation sensing by the NoCut checkpoint. *Nat Cell Biol* 2009; 11:477-83.
- Joglekar AP, Bouck DC, Molk JN, Bloom KS, Salmon ED. Molecular architecture of a kinetochore-microtubule attachment site. *Nat Cell Biol* 2006; 8:581-5.
- Meluh PB, Yang P, Glowczewski L, Koshland D, Smith MM. Cse4p is a component of the core centromere of *Saccharomyces cerevisiae*. *Cell* 1998; 94:607-13.
- Moore JK, Stuchell-Brereton MD, Cooper JA. Function of dynein in budding yeast: mitotic spindle positioning in a polarized cell. *Cell Motil Cytoskeleton* 2009; 66:546-55.
- Cervený KL, Studer SL, Jensen RE, Sesaki H. Yeast mitochondrial division and distribution require the cortical Num1 protein. *Dev Cell* 2007; 12:363-75.
- Deschenes RJ, Broach JR. Fatty acylation is important but not essential for *Saccharomyces cerevisiae* RAS function. *Mol Cell Biol* 1987; 7:2344-51.
- Finogold AA, Schafer WR, Rine J, Whiteway M, Tamanoi F. Common modifications of trimeric G proteins and ras protein: involvement of polyisoprenylation. *Science* 1990; 249:165-9.
- Srinivasa SP, Bernstein LS, Blumer KJ, Linder ME. Plasma membrane localization is required for RGS4 function in *Saccharomyces cerevisiae*. *Proc Natl Acad Sci USA* 1998; 95:5584-9.
- Eshel D, Urrestarazu LA, Vissers S, Jauniaux JC, van Vliet-Reedijk JC, Planta RJ, et al. Cytoplasmic dynein is required for normal nuclear segregation in yeast. *Proc Natl Acad Sci USA* 1993; 90:11172-6.
- Geiser JR, Schott EJ, Kingsbury TJ, Cole NB, Toris LJ, Bhattacharyya G, et al. *Saccharomyces cerevisiae* genes required in the absence of the CIN8-encoded spindle motor act in functionally diverse mitotic pathways. *Mol Biol Cell* 1997; 8:1035-50.
- Li YY, Yeh E, Hays T, Bloom K. Disruption of mitotic spindle orientation in a yeast dynein mutant. *Proc Natl Acad Sci USA* 1993; 90:10096-100.
- Lee WL, Kaiser MA, Cooper JA. The offloading model for dynein function: differential function of motor subunits. *J Cell Biol* 2005; 168:201-7.

31. Lee WL, Oberle JR, Cooper JA. The role of the lissencephaly protein Pac1 during nuclear migration in budding yeast. *J Cell Biol* 2003; 160:355-64.
32. Miller RK, Matheos D, Rose MD. The cortical localization of the microtubule orientation protein, Kar9p, is dependent upon actin and proteins required for polarization. *J Cell Biol* 1999; 144:963-75.
33. Miller RK, Rose MD. Kar9p is a novel cortical protein required for cytoplasmic microtubule orientation in yeast. *J Cell Biol* 1998; 140:377-90.
34. Sheeman B, Carvalho P, Sagot I, Geiser J, Kho D, Hoyt MA, et al. Determinants of *S. cerevisiae* dynein localization and activation: implications for the mechanism of spindle positioning. *Curr Biol* 2003; 13:364-72.
35. Desrivieres S, Cooke FT, Parker PJ, Hall MN. MSS4, a phosphatidylinositol-4-phosphate 5-kinase required for organization of the actin cytoskeleton in *Saccharomyces cerevisiae*. *J Biol Chem* 1998; 273:15787-93.
36. Homma K, Terui S, Minemura M, Qadota H, Anraku Y, Kanaho Y, et al. Phosphatidylinositol-4-phosphate 5-kinase localized on the plasma membrane is essential for yeast cell morphogenesis. *J Biol Chem* 1998; 273:15779-86.
37. Stefan CJ, Audhya A, Emr SD. The yeast synaptonemal complex proteins control the cellular distribution of phosphatidylinositol (4,5)-bisphosphate. *Mol Biol Cell* 2002; 13:542-57.
38. Moore JK, Sept D, Cooper JA. Neurodegeneration mutations in dynactin impair dynein-dependent nuclear migration. *Proc Natl Acad Sci USA* 2009; 106:5147-52.
39. Yeh E, Skibbens RV, Cheng JW, Salmon ED, Bloom K. Spindle dynamics and cell cycle regulation of dynein in the budding yeast, *Saccharomyces cerevisiae*. *J Cell Biol* 1995; 130:687-700.
40. Yeh E, Yang C, Chin E, Maddox P, Salmon ED, Lew DJ, et al. Dynamic positioning of mitotic spindles in yeast: role of microtubule motors and cortical determinants. *Mol Biol Cell* 2000; 11:3949-61.
41. Vorvis C, Markus SM, Lee WL. Photoactivatable GFP tagging cassettes for protein-tracking studies in the budding yeast *Saccharomyces cerevisiae*. *Yeast* 2008; 25:651-9.
42. Longtine MS, McKenzie A, 3rd, Demarini DJ, Shah NG, Wach A, Brachat A, et al. Additional modules for versatile and economical PCR-based gene deletion and modification in *Saccharomyces cerevisiae*. *Yeast* 1998; 14:953-61.
43. Sikorski RS, Hieter P. A system of shuttle vectors and yeast host strains designed for efficient manipulation of DNA in *Saccharomyces cerevisiae*. *Genetics* 1989; 122:19-27.
44. Kanoksilapatham W, Gonzalez JM, Robb FT. Directed-Mutagenesis and Deletion Generated through an Improved Overlapping-Extension PCR Based Procedure. *Silpakorn U Science & Tech J* 2007; 1:7-12.

©2009 Landes Bioscience.
Do not distribute.